

## Polyoxotungstate Incorporating Organotriphosphonate Ligands: Synthesis, Characterization, and Catalytic for Alkene Epoxidation

Yu Huo, Zhiyuan Huo, Pengtao Ma, Jingping Wang,\* and Jingyang Niu\*

Key Laboratory of Polyoxometalate Chemistry of Henan Province, College of Chemistry and Chemical Engineering, Henan University, Kaifeng 475004, P. R. China

## Supporting Information

**ABSTRACT:** A S-shaped organotriphosphonate polyoxotungstate,  $K_4H_6[H_4\{(AsW_9O_{33})Zn(H_2O)W_5O_{11}(N(CH_2PO_3)_3)\}_2(\mu_2-O)_2]\cdot 27H_2O$  (**1**), has been synthesized and characterized. Compound **1** contains a different geometry of  $[\{Zn(H_2O)W_5O_{19}(N(CH_2PO_3)_3)\}]^{12-}$  clusters, which forms a chiral conformation. The catalysis of **1** for alkene epoxidation was investigated with a hydrogen peroxide ( $H_2O_2$ ) oxidant.

Organophosphonate-based polyoxometalate (POM) derivatives have been growing in leaps and bounds in recent years due to their great diversity in size, nuclearity, and shape, as well as their promising applications in catalysis, electrochemistry, photochromism, magnetism, and medicine.<sup>1</sup> To date, the crystallographic structures of the reaction products of  $Mo^{VI}$  and  $V^V$  ions with bisphosphonates have been widely discovered and fully explored on account of their potential properties,<sup>2</sup> which are further modified by transition metals (TM) combining with organic linkers to generate high dimensional structures.<sup>3</sup> Whereas, the development of organophosphonate-decorated polyoxotungstates is sluggish, which may be due to the inactivity of the reaction system of W and organophosphonate. The first example of polyoxotungstate containing a functionalized diphosphonate is Pope's  $[(O_3P-CH_2-PO_3)_4W_{12}O_{36}]^{16-}$ , which was reported in 1994.<sup>4</sup> Since then, only a series of the organophosphonic acid derivatives were grafted on the Keggin tungstate anions  $[PW_9O_{34}]^{9-}$  and  $[\gamma-SiW_{10}O_{36}]^{4-}$ , as well as Lindqvist  $[NbW_5O_{19}]^{3-}$ . The only example of TM-substituted organodiphosphonate-based polyoxotungstate,  $[\{(B-\alpha-PW_9O_{34})Co_3(OH)(H_2O)_2(O_3PC(O)-(C_3H_6NH_3)PO_3)\}_2Co]^{14-}$ , was reported by Mialane, Dolbecq, and co-workers until 2012.<sup>5</sup>

A survey of the available literatures shows that tungsten compounds are active, and selective catalysts for olefin epoxidation<sup>6</sup> and the catalytic reactions can be significantly increased by the incorporation of organic and organometallic groups.<sup>7</sup> Therefore, we focus on the synthesis of novel polyoxotungstate structures based on organophosphonate and hope to discover good efficiency and selectivity in the catalytic oxidation of alkenes. Among the reported organophosphonate ligands, the design and synthesis of triphosphonate-POMs are extremely limited. Only two examples including the triphosphonate ligand are a two-dimensional trinuclear  $[V_3O_3(OH)-\{C_6H_3(C_6H_4PO_3H)_3\}]$  cluster and one crown-shaped polyoxomolybdate  $Na_5[H_7\{N(CH_2PO_3)_3\}Mo_6O_{16}(OH)(H_2O)_4]^{4-}$

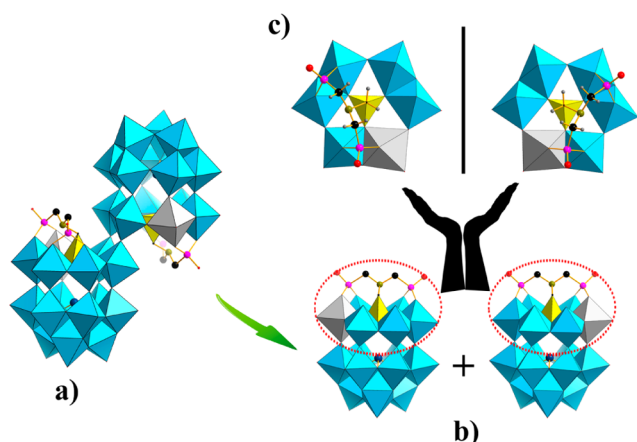
$18H_2O$ ,<sup>8</sup> while no triphosphonate-based polyoxotungstate has been discovered. The amino trimethylene phosphonic acid (ATMP) has our attention for the following advantages: (a) It is stable over a wide range of temperatures and pH values.<sup>9</sup> (b) It is flexible in space morphology, which has benefits for coordination. (c) It is a nontoxic and multidentate ligand, which provides an impetus for the synthesis of diverse structures and functional materials. In addition, the precursor dilacunary  $[As_2W_{19}O_{67}(H_2O)]^{14-}$  should be an ideal building block because of the bridging  $\{WO(H_2O)\}$  linker in the precursor providing a fracture point where the molecule can be disassembled and may rearrange during the course of the reaction.<sup>10</sup>

Herein, we report the synthesis and characterization of a zinc-containing ATMP-based POM derivative  $K_4H_6[H_4\{(AsW_9O_{33})Zn(H_2O)W_5O_{11}(N(CH_2PO_3)_3)\}_2(\mu_2-O)_2]\cdot 27H_2O$  (**1**), which presents the first example of incorporating functionalized triphosphonates into polyoxotungstate. Furthermore, giving the presence of both ATMP ligands and Zn ions in the same polyanion, the catalytic oxidation of olefin has been preliminary studied.

Colorless block-shaped crystals of **1** were obtained by a one-pot reaction of the precursor  $[As_2W_{19}O_{67}(H_2O)]^{14-}$ , organotriphosphonate ligand ATMP, and  $ZnCl_2$ . The phase purity of **1** was confirmed using X-ray powder diffraction (Figure S5, Supporting Information). Single-crystal X-ray structural analysis indicated that **1** crystallizes in the monoclinic space group  $C2/c$ . As shown in Figure 1,  $[\{(AsW_9O_{33})Zn(H_2O)W_5O_{11}(N(CH_2PO_3)_3)\}_2(\mu_2-O)_2]^{14-}$  (**1a**) can be viewed as two Zn-substituted trivacant Well–Dawson  $[\{(AsW_9O_{33})M(H_2O)W_5O_{11}(N(CH_2PO_3)_3)\}(\mu_2-O)_2]^{9-}$  building blocks in opposite directions that are connected by two  $\mu_2$ -oxo groups acting as the “hinge”, giving the anion a S-shaped structure. The Well–Dawson structure contains a trilacunary fragment  $[\alpha-AsW_9O_{33}]^{9-}$  and a triangular ring-like cluster  $[\{Zn(H_2O)W_5O_{19}(N(CH_2PO_3)_3)\}]^{12-}$  fused together by six corner-sharing  $\mu_2$ -O atoms. An intriguing structural feature of **1** is the two ring-like fragments presenting a different geometry between them, which has a chiral conformation (Figure 1c). The fragment contains a central tetrahedral  $\{PO_3C\}$  group encircled by a ring of five  $\{WO_6\}$  and an extra  $\{ZnO_6\}$  octahedra sharing edges and corners alternately, which is similar to the well-known polyoxoanion  $[Mo_7O_{16}(O_3PCH_2PO_3)_3]^{8-}$ .<sup>11</sup> The central P atom coordinates to three  $\mu_3$ -O atoms, which

Received: September 30, 2014

Published: December 29, 2014



**Figure 1.** (a) Combined polyhedral/ball-and-stick representation of **1a**. (b) Combined polyhedral/ball-and-stick representation of the subunit. (c) Chiral conformation of the ring-like clusters. Color code: As, dark blue; C, black; H, gray-50%; N, dark yellow; P, pink;  $\text{PO}_3\text{C}$  tetrahedral, yellow;  $\text{WO}_6$  octahedral, sky blue; and  $\text{ZnO}_6$  octahedral, gray-25%.

anchors to two M atoms ( $M = \text{W}, \text{Zn}$ ). The other two P atoms of ATMP separately connect with two  $\{\text{MO}_6\}$  octahedra via two  $\mu_2$ -oxo groups, which are exposed on the outside of the ring. As reported previously,<sup>8b</sup> ATMP plays an important role in the stabilization of metal-substituted POMs. Additionally, the C1 atom, center P atom, and As<sup>III</sup> heteroatom are almost linear with the C–P–As angle of  $176.74^\circ$  (Figure S2, Supporting Information).

According to the bond valence sum (BVS) calculations,<sup>12</sup> the oxidation states of the As, P, W, and Zn atoms are +3, +3, +6, and +2, respectively, and the results of P and W are further confirmed by XPS spectra (Figure S14, Supporting Information). In the ring-like polyanion, the Zn atom is coordinated to a single terminal aqua ligand and has two Zn–O–P with angles of  $128.0(8)^\circ$  and  $131.0(9)^\circ$ , which also possesses three Zn–O–W linkages with angles in the range of  $89.8(5)$ – $159.5(1)^\circ$ . The P atoms connect with M atoms through  $\mu_2$ -oxo and  $\mu_3$ -oxo groups; thus, the O–P–C bond angles, O–P–O angles, and P–O–W lie in the range of  $99.4(9)$ – $110.0(9)^\circ$ ,  $109.3(8)$ – $115.9(8)^\circ$  and  $131.9(8)$ – $138.8(8)^\circ$ . As expected, the As<sup>III</sup> atoms appear with trigonal-pyramid coordination geometry with the As–O bonds ranging between 1.776(13) and 1.808(15) Å. Furthermore, the structure of **1a** is extended to a two-dimensional layerwork structure by the coordination of four additional  $\text{K}^+$  cations (Figure S4, Supporting Information).

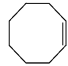
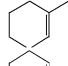

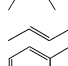
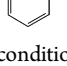
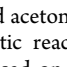
NMR spectroscopy was studied on the compound in order to investigate the solution stability of the polyanion. The  $^{31}\text{P}$  NMR spectrum of the fresh solution of **1** in  $\text{D}_2\text{O}$  (700  $\mu\text{L}$ ) exhibits two doublets and two single peaks (Figure S6, Supporting Information). The result may contain two sets of signals, which is probably a mixture of isomers, that is,  $\Lambda$ – $\Lambda$ ,  $\Delta$ – $\Delta$ -type, and  $\Delta$ – $\Lambda$ ,  $\Lambda$ – $\Delta$ -type. The single peaks belong to the central P atoms, and the doublets are attributed to the peripheral P atoms (Figure S7, Supporting Information). In order to study this equilibrium in solution,  $^{31}\text{P}$  NMR spectra at different pH values ranging between 1.0 and 5.8 were observed. We observed that in the range of pH 1.0–1.6, the compound has partially decomposed. When the pH values ranges between 2.2 and 3.4, the presence of the two sets were observed. Upon increasing the pH to 4.6, three resonances located at 3.86, 8.74, and 11.13 ppm faded away. When the pH value increased to

5.2, only one set of three peaks ( $\delta = 2.68, 8.57, 10.86$  ppm) was observed (Figure S8, Supporting Information). In the presence of  $\text{Li}^+$  and  $\text{Na}^+$ , only the other set of three single peaks remained at 3.86, 8.74, and 11.13 ppm in the  $^{31}\text{P}$  NMR spectra.

In order to explore the electrochemical behaviors of **1**, cyclic voltammetry studies were carried out in a pH 3 sulfate medium (0.2 M  $\text{Na}_2\text{SO}_4 + \text{H}_2\text{SO}_4$ ) where **1** was stable at  $150 \text{ mV s}^{-1}$  scan rate. The electrochemical properties of the product were investigated in the potential range of 0.3 V to approximately  $-1.0$  V. Three W-based waves were observed with their reduction peak potentials located at  $-0.39, -0.55,$  and  $-0.71$  V vs SCE, respectively. The redox peaks could be assigned to three consecutive two-electron processes of W.<sup>13</sup> The peak potential differences of three couples of redox waves are 60, 62, and 56 mV, respectively, indicating that they are one-electron charge-transfer processes. In addition, the peak currents related to the tungsten redox processes were proportional to the square root of the scan rate in the range of  $80$ – $300 \text{ mV s}^{-1}$ , suggesting that redox processes are diffusion controlled.<sup>13</sup>

As known, use of organic–inorganic hybrid polyoxotungstates has been recently proposed as a catalyst upgrade.<sup>14</sup> Compared to the nonfunctionalized POMs, the phosphonate derivative displays an improved thermal stability and a wide substrate scope.<sup>15</sup> Thus, we explored the catalytic reaction of **1**, the initial experimental procedure for the epoxidation reaction by using cyclohexene as a model substrate with 2 equiv of  $\text{H}_2\text{O}_2$ . Under optimal conditions, cyclohexene was oxidized to the expected 1,2-epoxycyclohexane with high conversion (94.1%) and excellent selectivity (>99%) (Table 1, entry 3).

**Table 1.** Epoxidation of Alkenes with  $\text{H}_2\text{O}_2$ <sup>a</sup>

Entry	Substrate	Time (h)	Temp. ( $^\circ\text{C}$ )	Conv. (%) <sup>d</sup>	Sel. (%)
1		4	75	50.6	
2		6	75	75.3	
3		8	75	94.1	
4		8	65	79.5	>99
5		8	55	29.3	
6 <sup>b</sup>		8	75	68.1	
7 <sup>c</sup>		8	75	21.0	
8		44	60	90.4	40.7
9		44	60	92.8	23.3
10		16	75	74.6	81.5
11		24	75	91.7	76.7
12		30	75	98.6	51.2

<sup>a</sup>Reaction conditions: catalyst (1  $\mu\text{mol}$ ), substrate (1 mmol),  $\text{H}_2\text{O}_2$  (2 mmol), and acetonitrile (5 mL). <sup>b</sup>Filtered catalyst. <sup>c</sup>Solution at the end of a catalytic reaction. <sup>d</sup>Determined by gas chromatography (GC) analyses based on initial substrate.

As shown in Table 1, the conversions remarkably declined (entries 1–5), which demonstrated that both the reaction time and temperature were the key factors that influence the conversion of epoxidation products. A blank experiment without **1** (Table S5, Supporting Information) indicated that the epoxidation would not occur. In contrast to catalyst **1**, the epoxidation reactions with the precursor  $\{\text{As}_2\text{W}_{19}\text{O}_{67}(\text{H}_2\text{O})\}$  and subunit  $\{\text{AsW}_9\text{O}_{33}\}$  indicated that the conversion was only

41.2% and 50.7%, respectively. After oxidation was completed, the catalyst could be retrieved from the solvent/oxidant/substrate system by filtration. When the reaction was carried out with the filtered catalyst, the conversion of cyclohexene was low (68.1%) after 8 h of reaction (entry 6). The epoxidation reaction with the solution at the end of a catalytic reaction gave 21% conversion (entry 7), which corresponded to the loss of catalytic activity (26%) after the first run. In order to investigate the stability of the catalyst,  $^{31}\text{P}$  NMR and IR spectra of the used catalyst have been studied. The  $^{31}\text{P}$  NMR spectrum only contains two single peaks at 2.73 and 3.90 ppm attributed to the central P atoms, indicating that the peripheral P atoms fall off. The noticeable differences of the IR spectrum are in the region between 1250 and 1500  $\text{cm}^{-1}$ . The results suggested that the framework structure of the catalyst was partially decomposed, and the skeleton of POMs was still retained. In the cases of other cyclic alkenes (entries 8–9), 1-methylcyclohexene gave 90.4% conversion and 40.7% selectivity. The catalyst system was applicable to aliphatic alkenes or aromatic alkenes (entries 10–12), with selectivity of 2,3-dimethyl-2-butene and trans-2-octene reaching to 81.5% and 76.7%, respectively.

In summary, the S-shaped, zinc-containing, polyoxotungstate-incorporated ATMP has been synthesized by a simple one-pot reaction. Compound **1** presents the first example of incorporating functionalized triphosphonates into polyoxotungstate rather than simply grafted on the surface. The catalysis of **1** for alkene epoxidation has been investigated with a hydrogen peroxide ( $\text{H}_2\text{O}_2$ ) oxidant in acetonitrile. The next work will concentrate on improving the activity and selectivity for alkene epoxidation and the synthesis of the isostructural derivatives with replacing the zinc atoms.

## ■ ASSOCIATED CONTENT

### ■ Supporting Information

X-ray crystallographic files (CIF), experiment sections, synthetic discussion, additional physical measurements, catalytic properties, and additional structural figures for **1**. This material is available free of charge via the Internet at <http://pubs.acs.org>.

## ■ AUTHOR INFORMATION

### Corresponding Authors

\*E-mail: [jpwang@henu.edu.cn](mailto:jpwang@henu.edu.cn) (J.W.) .

\*E-mail: [jyniu@henu.edu.cn](mailto:jyniu@henu.edu.cn) (J.N.) .

### Notes

The authors declare no competing financial interest.

## ■ ACKNOWLEDGMENTS

We gratefully acknowledge the National Natural Science Foundation of China, Foundation of Education Department of Henan Province, and Natural Science Foundation of Henan Province for financial support.

## ■ REFERENCES

- (1) (a) Pope, M. T.; Muller, A. *Angew. Chem., Int. Ed.* **1991**, *30*, 34–38. (b) Hill, L. M. R.; Abrahams, B. F.; Young, C. G. *Chem.—Eur. J.* **2008**, *14*, 2805–2810. (c) Zhang, Y.; Cao, R.; Guo, R. T.; Robinson, H.; Papapoulos, S.; Wang, A. H.; Kubo, T.; Oldfield, E. *J. Am. Chem. Soc.* **2009**, *131*, 5153–5162. (d) Long, D. L.; Tsunashima, R.; Cronin, L. *Angew. Chem., Int. Ed.* **2010**, *49*, 1736–1758.
- (2) (a) Dolbecq, A.; Mialane, P.; Sécheresse, F.; Keita, B.; Nadjjo, L. *Chem. Commun.* **2012**, *48*, 8299–8316. (b) Banerjee, A.; Bassil, B. S.; Rösenthaler, G.-V.; Kortz, U. *Chem. Soc. Rev.* **2012**, *41*, 7590–7604.

(c) Niu, J. Y.; Zhang, X. Q.; Yang, D. H.; Zhao, J. W.; Ma, P. T.; Kortz, U.; Wang, J. P. *Chem.—Eur. J.* **2012**, *18*, 6759–6762.

(3) (a) Burgomaster, P. D.; Aldous, A.; Liu, H. X.; O'Connor, C. J.; Zubieta, J. *Cryst. Growth Des.* **2010**, *10*, 2209–2218. (b) Li, F. Y.; Xu, L. *Dalton Trans.* **2011**, *40*, 4024–4034. (c) Shestakova, P.; Absillis, G.; Martin-Martinez, F. J.; Proft, F. D.; Willem, R.; Parac-Vogt, T. N. *Chem.—Eur. J.* **2014**, *20*, 5258–5270.

(4) Kortz, U.; Jameson, G. B.; Pope, M. T. *J. Am. Chem. Soc.* **1994**, *116*, 2659–2660.

(5) (a) Mayer, C. R.; Herson, P.; Thouvenot, R. *Inorg. Chem.* **1999**, *38*, 6152–6158. (b) Kortz, U.; Marquer, C.; Thouvenot, R.; Nierlich, M. *Inorg. Chem.* **2003**, *42*, 1158–1162. (c) Mayer, C. R.; Hervé, M.; Lavanant, H.; Blais, J. C.; Sécheresse, F. *Eur. J. Inorg. Chem.* **2004**, *5*, 973–977. (d) Driss, H.; Boubekeur, K.; Debbabi, M.; Thouvenot, R. *Eur. J. Inorg. Chem.* **2008**, *23*, 3678–3686. (e) Moll, H. E.; Dolbecq, A.; Marrot, J.; Rousseau, G.; Haouas, M.; Taulelle, F.; Rogez, G.; Wernsdorfer, W.; Keita, B.; Mialane, P. *Chem.—Eur. J.* **2012**, *18*, 3845–3849. (f) Moll, H. E.; Rousseau, G.; Dolbecq, A.; Oms, O.; Marrot, J.; Haouas, M.; Taulelle, F.; Rivière, E.; Wernsdorfer, W.; Lachkar, D.; Lacôte, E.; Keita, B.; Mialane, P. *Chem.—Eur. J.* **2013**, *19*, 6753–6765.

(6) (a) Lane, B. S.; Burgess, K. *Chem. Rev.* **2003**, *103*, 2457–2473. (b) Noyori, R.; Aoki, M.; Sato, K. *Chem. Commun.* **2003**, *16*, 1977–1986. (c) Mizuno, N.; Yamaguchi, K.; Kamata, K. *Coord. Chem. Rev.* **2005**, *249*, 1944–1956. (d) Maksimchuk, N. V.; Kovalenko, K. A.; Arzumanov, S. S.; Chesalov, Y. A.; Melgunov, M. S.; Stepanov, A. G.; Fedin, V. P.; Kholdeeva, O. A. *Inorg. Chem.* **2010**, *49*, 2920–2930.

(7) (a) Marcoux, P. R.; Hasenknopf, B.; Vaissermann, J.; Gouzerh, P. *Eur. J. Inorg. Chem.* **2003**, *13*, 2406–2412. (b) Santoni, M. P.; Pal, A. K.; Hanan, G. S.; Proust, A.; Hasenknopf, B. *Inorg. Chem.* **2011**, *50*, 6737–6745. (c) Lin, C. G.; Chen, W.; Long, D. L.; Cronin, L.; Song, Y. F. *Dalton Trans.* **2014**, *43*, 8587–8590.

(8) (a) Ouellette, W.; Wang, G. B.; Liu, H. X.; Yee, G. T. *Inorg. Chem.* **2009**, *48*, 953–963. (b) Yang, L.; Ma, P. T.; Zhou, Z.; Wang, J. P.; Niu, J. Y. *Inorg. Chem.* **2013**, *52*, 8285–8287.

(9) (a) Tantayakom, V.; Fogler, H. S.; Charoensirithavorn, P.; Chavade, S. *Cryst. Growth Des.* **2005**, *5*, 329–335. (b) Ruiz-Agudo, E.; Putnis, C. V.; Rodriguez-Navarro, C. *Cryst. Growth Des.* **2008**, *8*, 2665–2673.

(10) (a) Ritchie, C.; Boskovic, C. *Cryst. Growth Des.* **2010**, *10*, 488–491. (b) Ritchie, C.; Speldrich, M.; Gable, R. W.; Sorace, L.; Kögerler, P.; Boskovic, C. *Inorg. Chem.* **2011**, *50*, 7004–7014. (c) Ritchie, C.; Baslon, V.; Moore, E. G.; Reber, C.; Boskovic, C. *Inorg. Chem.* **2012**, *51*, 1142–1151.

(11) Dumas, E.; Sassoie, C.; Smith, K. D.; Sevov, S. C. *Inorg. Chem.* **2002**, *41*, 4029–4032.

(12) Brown, I. D.; Altermatt, D. *Acta Crystallogr. Sect. B* **1985**, *41*, 244–247.

(13) (a) Bassil, B. S.; Ibrahim, M.; Mal, S. S.; Suchopar, A.; Biboum, R. N.; Keita, B.; Nadjjo, L.; Nellutla, S.; Tol, J. V.; Dalal, N. S.; Kortz, U. *Inorg. Chem.* **2010**, *49*, 4949–4959. (b) Nambu, J. I.; Ueda, T.; Guo, S. X.; Boasc, J. F.; Bond, A. M. *Dalton Trans.* **2010**, *39*, 7364–7373. (c) Gabb, David.; Pradeep, C. P.; Miras, H. N.; Mitchell, S. G.; Long, D. L.; Cronin, L. *Dalton Trans.* **2012**, *41*, 10000–10005.

(14) (a) Bonchio, M.; Carraro, M.; Scorrano, G.; Bagno, A. *Ad. Synth. Catal.* **2004**, *346*, 648–654. (b) Berardi, S.; Carraro, M.; Sartorel, A.; Modugno, G.; Bonchio, M. *Isr. J. Chem.* **2011**, *51*, 259–274.

(15) (a) Carraro, M.; Sandei, L.; Sartorel, A.; Scorrano, G.; Bonchio, M. *Org. Lett.* **2006**, *8*, 3671–3674. (b) Berardi, S.; Bonchio, M.; Carraro, M.; Conte, V.; Sartorel, A.; Scorrano, G. *J. Org. Chem.* **2007**, *72*, 8954–8957.